What Lies Beyond Sight? Applications of Ultraportable Hyperspectral Imaging (VIS-NIR) for Archaeological Fieldwork

Claudia Sciuto, Federico Cantini, Rémy Chapoulie, Corentin Cou, Hortense de la Codre, Gabriele Gattiglia, Xavier Granier, Aurélie Mounier, Vincenzo Palleschi, Germana Sorrentino, et al.

What lies beyond sight. Applications of ultraportable hyperspectral imaging (VIS-NIR) for archaeological fieldwork

Claudia Sciuto[1], Federico Cantini[1], Rémy Chapoulie[2], Corentin Cou[3], Hortense De la Codre[2], Gabriele Gattiglia[1], Xavier Granier[3], Aurélie Mounier[2], Vincenzo Palleschi[5], Germana Sorrentino[1], Simona Raneri[5]

[1] Department of Civilisations and Forms of Knowledge, University of Pisa, Italy

[2] Archéosciences Bordeaux UMR 6034 CNRS, University Bordeaux Montaigne

[3] LP2N UMR 5298 & Inria Bordeaux Sud-Ouest & InVisu USR 3103, CNRS

[4] LP2N UMR 5298, Institut d'Optique Graduate School

[5] ICCOM-CNR, National Research Council, Pisa, Italy

Abstract

Hyperspectral imaging is a widespread non-destructive analytical technique used in various disciplines for highlighting invisible patterns and mapping the spectral signatures of selected targets. In archaeology, it has been mostly applied for remote sensing satellite imagery to disclose information about features that are hidden undergrounds. Targeted applications of hyperspectral imaging have been developed in the last few years, opening up new perspectives for material analysis based on spectral mapping. Recent advances in portable instrumentation have led to the development of small and rugged cameras that can be used directly in the field for investigating different targets. This paper discusses the use of a small ultraportable hyperspectral camera in the VIS-NIR range for archaeological fieldwork with regards to hardware, data processing workflows, and spectral information that can be used for the better planning of research and for *in situ* screening.

1. Introduction

In the last ten years, the fast evolution of portable analytical techniques has supported the development of protocols for highlighting invisible properties of the archaeological record directly in the field. The availability of instruments produced as "rugged" devices, that can be transported and used in various conditions (such as XRF or Raman spectrometers), has fostered the evolution of interdisciplinary approaches to fieldwork (Milek 2018; Vandenabeele & Donais 2016). The combination of different techniques is essential to unlock information hidden in the archaeological record and, within the wide toolset of portable instruments, the particular interest in hyperspectral imaging applications lies especially in its flexibility as a fast-mapping method.

Hyperspectral imaging (therein HSI) in the spectral region from the Near ultraviolet (NUV) to the Near Infrared range (NIR) is a well-known technique applied in routine analysis in different scientific and industrial fields, from pharmaceutics to agriculture, from food production to geology. Many successful

applications of HSI have inspired the use of this technique in archaeology, where imaging has been applied to a variety of targets. During the last ten years, following the leading experiences in art history and, more broadly, cultural heritage conservation, applications of HSI in targeted research started developing for the field of archaeology. The first and most common applications of HSI in archaeological research are those as untargeted remote sensing method, through the analysis of aerial and satellite data, where image analysis is based on the interpretation of proxy information that can help pinpointing buried evidence (among many others, see the outstanding examples of Campana & Forte, 2006; Masini & Soldovieri 2017; Parcak 2009).

The widespread application of hyper and multi-spectral imaging in art history is aimed at retracing the steps of the artistic craft, highlighting hidden patterns in paintings (Cucci, Delaney, & Picollo 2016; Liang 2012). The combination of Hyper- and Multispectral Imaging with advanced statistical treatments of the hyperspectral set has led to the development of the MHX (Multi-Illumination Hyperspectral eXtraction) technique (Salerno et al., 2014; Triolo et al., 2020) which has produced remarkable results in bringing back to the light paintings and pictorial traces otherwise invisible and lost (Adinolfi et al., 2019; Legnaioli et al., 2013a). Spectral fingerprints can also be used to identify pigments recipes and map their distribution on painted surfaces (Cucci et al. 2020). HSI in the Vis-NIR range can detect pigments and dyes on fragile materials such as miniatures, engravings, tapestries, paintings (Cucci, Delaney, & Picollo 2016; Gabrieli et al. 2019; Mounier et al., 2016; 2017; 2018) and as an exploratory method for highlighting similarities or dissimilarities in the composition of materials and setting sampling strategies for further elemental analysis.

HSI has been applied as a field and laboratory screening technique for provenance studies, where the classification of rock types, based on their spectral signature, has been proven to be an effective method for clustering raw materials used in construction or lithic tools (Parish 2011; Sciuto et al. 2018; 2019). Rather accurate classification of minerals can be done on the SWIR (Short-wave infrared) range, covering the band up to 2500 nm. NIR and VIS spectroscopy has also been adopted to determine heat treatment in silica rocks (Schmidt et al. 2013) and identify traces of organic residues (Prinsloo et al. 2008). Applications of NIR spectroscopy and imaging have been tested for the study of soils and sediments in the archaeological record. Specific materials, such as bone fragments, can be easily identified and mapped through image analysis while assessing their preservation state (Linderholm et al. 2013). Furthermore, through specific statistical processing, image analysis can help classify sediments in profiles, gathering information on depositional and post-depositional processes (Choi et al. 2020; Linderholm et al. 2019).

Light, portable, and quick image-based techniques enable the spectral mapping and the total coverage of geochemical information on a surface. This characteristic of HSI facilitates the simultaneous investigation of a considerable number of artefacts as well as the mapping of wide surfaces, with the

fast gathering of large datasets (Koehler et al. 2002). These specific features that characterise imaging techniques become particularly useful when dealing with most archaeological case studies. When working on excavations, geochemical data could be collected directly at "the trowel's edge" (Hodder & Berggren 2005) simply by taking a photograph. The extreme portability of some hyperspectral devices could also represent an advantage for surveys, where the instruments is carried directly in the field and used when needed, thus integrating the routine documentation of observed features. Nevertheless, the miniaturisation of sensors in small and portable devices could lead to reducing both spatial and spectral resolution. Therefore, it is important to be fully aware of the limits of single instruments and processing pipelines to obtain the best results with the available data. Spectral datasets provide unbiased information about artefacts that could substitute optical observations, speeding up the research process both in the field and in a laboratory. Nonetheless, the interpretation of spectral signatures could be made difficult by the presence of overlapping peaks and the scarce availability of references libraries of specific archaeological materials, which can sometimes be covered by data reported in individual publications or general online libraries (Baldridge et al. 2009; Clark et al. 1993; Rossel et al. 2016). For this reason, a fingerprint approach is often preferable for image mapping, where certain spectral bands can be considered as characteristic of specific materials and help understanding the nature of the target. In other cases, proxies that are linked to the target morphology, such as grain size or moisture, can be a valuable help to pinpoint some physical characteristics of materials that would otherwise be invisible.

The application of HSI to different study targets has originated a fair number of methodological papers, but while the literature on selected case studies is vast, the use of HSI has rarely been effectively implemented in archaeological research routine. The aim of this paper is to provide a survey of common archaeological research cases, in which a compact ultraportable HSI camera (©Specim IQ hyperspectral camera) has been used, with practical descriptions of acquisition setups, data processing workflows and spectral responses of materials in the VIS-NIR region. The specific instrument has been chosen because it fulfils the requirements mentioned above in terms of portability, ease of usage, and stability. By outlining data acquisition setups and evaluating the data collected, we will highlight potentials and issues with the application of ultraportable HSI for understanding the archaeological record and various types of findings. By providing a set of hands-on protocols, we wish to encourage experimentation with hyperspectral cameras applications in routine fieldwork activities.

2. HSI device and data processing

The examples herewith presented have been analysed using the IQ camera by Specim, commercially presented as the first ultraportable compact hyperspectral camera. The instrument – mainly employed for agriculture and food analysis applications (Behman et al., 2017) - has been recently proposed for

Cultural Heritage and archaeological applications. The camera weighs 1.3 kg and measures 207 x 91 x 74 mm. The images are acquired through a CMOS sensor, covering a wavelength range between 400 and 1000 nm, with a spectral resolution of 7 nm and a spatial resolution of 512 x 512 pixels per image. The camera can be used both indoor and outdoor, using controlled lighting with halogen lamps or acquiring images in full sunlight. Calibration is performed against a Spectralon tile that must be positioned close to the target when acquiring images. The IQ camera software allows the recording of white reference data in one image while saving it for the following acquisitions, particularly useful in controlled lighting environments. After processing the monochromatic images of the datacube, the final hyperspectral image is reconstructed, each pixel containing the reflectance spectrum of the corresponding point of the object.

Hyperspectral imaging provides more information than RGB imaging in the context of automatic image processing. RGB imaging suffers from metamerism: different spectra, when reduced to the three fundamental bands of Blue, Green and Red, may result in an identical RGB colour. In fact, two different materials may have the same colour but a different spectrum. While it would be impossible to differentiate the two materials automatically on an RGB image, the process can be done by adding more spectral information within a set of hyperspectral images. Hyperspectral remote sensors may collect image data in hundreds of narrow, adjacent spectral bands, giving an almost continuous spectrum for each image pixel. The reflectance spectra acquired with an HSI camera can be treated to obtain conventional images (RGB or False-Color Infrared), or more advanced statistical treatment can be applied, such as Chromatic Derivative (ChromaDI, Legnaioli et al., 2013b), True-Color Infrared (Grifoni, 2019) or Multi-illumination Hyperspectral eXtraction (MHX, Triolo et al., 2020).

Images acquired by HSI ultraportable camera often result in heavy files that can be processed through different approaches, software, and routines to reach diverse levels of data analysis. The IQ studio Specim software is free for download on the company's website, but it provides just a few tools for exploring the spectral information in the hyperspectral set. For most practical applications, the user is forced to move to third party software or programming their own routines.

Processing information delivered by HSI requires specific stages that can be batched in order to reduce the size of the files without losing spectral accuracy. Multivariate Image Analysis (MIA) is the most common procedure for treating multi- and hyperspectral images. Every picture is divided into a system of x and y coordinates depending on the number of pixels contained in the file, while z is determined, in our case, by the spectral bands (in wavelengths) covered by the device. Image treatment consists of reducing the spectral information by highlighting the relationships between variables and contracting the dataset (Geladi & Grahn, 1996; Grahn & Geladi, 2007). Images can be analysed by considering information associated with single pixels or evaluating the entire image (Prats-Montalbán, et al., 2011). The most common MIA model is PCA, which is calculated on the entire data matrix. The image is

visualised as a colour composite, and a new value is associated with each pixel according to the information highlighted by the PCA components. Evince, by Prediktera, is a commercial software created for multivariate analysis on hyperspectral images. An intuitive interface allows data mining by means of supervised and unsupervised clustering algorithms, useful for a first exploration of the data and information reduction operations.

Another possible solution is processing the images with a programming workflow. For example, some libraries like Spectral Python allow the import of spectral images in ENVI format (ENVI, 2005). Images are converted into 3D-arrays and can therefore be processed with the same algorithms as conventional image processing. In most cases, Python routines enable quickly reach of some hardware limits, while the main advantage of Python workflows is the possibility of applying modifications to the image before analysing the spectra. Here are some examples of possible image processing in Python:

- *Shadow correction:* The Specim IQ camera is portable and allows acquisitions to be made in uncontrolled environments. Light sources can be a problem when collecting measurements outdoors. The illuminance of the scene can be inhomogeneous, causing shadows in the image obtained that can be corrected in pre-processing to obtain usable spectra. In the case of a simple image, the correction can be done by determining the illuminance of the scene, i.e. the light intensity, for each pixel of the image, calculating the integral of the spectrum in the visible (400-800 nm).

- *Automatic detection:* A Python workflow is not limited to the pre-processing of the image or its observation; in fact, it is also possible to automatically detect a specific spectral signal, for example, related to a pigment.

The advantage of applying a Python workflow is its great versatility, as the workflow can easily be adapted from case to case, depending on the image and the research goal.

Both Python workflows and modelling with Evince can be easily done directly in the field, thus evaluating the image quality while acquiring data. Image acquisition can take up to a few minutes, but it is usually very fast. A quick assessment of data files on a laptop can be helpful in order to collect better information and get geochemical data on selected targets while conducting the research.

3. Case studies

The case studies were selected in order to cover a wide range of materials and contexts in which HSI could be applied to detect invisible patterns and support the interpretation of archaeological features.

3.1 Soil profile and masonries

The ongoing research project carried out in the courtyard nearby the Medieval church of San Sisto in Pisa is aimed at investigating an area of the city where scholars have traditionally placed the seat of public power between the Langobard period (7th century) and the beginning of the 11th century. Since

2020, the project managed by the Department of Civilisations and Forms of Knowledge of the University of Pisa (Italy) involves the dig of the church courtyard as well as the analysis of vertical stratigraphy of the building's medieval masonries. The research site was the occasion for testing the use of HSI for a fast mapping and classification of soil profiles to map the layers based on soil proxies such as texture and humidity and building materials in masonries, based on their spectral responses. The IQ camera was mounted on a tripod and used directly outdoor on the working site. Acquisitions were made in full sunlight with the camera positioned at about 2 m from the soil profile and about 5 meters from the masonries. The hyperspectral data obtained were processed using Evince software (Prediktera), which allowed a quick evaluation of the acquired spectra and the processing of several multivariate statistical models on the set of recorded information. The calculation of a model for data reduction, the computation of a principal components analysis model (PCA), provided an overview of the spectral characteristics of the investigated subjects.

As mentioned above, the spectral signature of most minerals cannot be found within the bandwidth recorded by the IQ camera. Nevertheless, some important information about sediments and the formation processes of the record can be inferred by looking at proxies such as soil moisture, the presence of organic material, soil morphology and grain size. The Evince processing of the images obtained with the IQ camera allows highlighting the (hyper-) colour variations and associating them to the corresponding VIS-NIR spectra to assist the observations conducted in the field by archaeologists. The comparison between RGB photography and the PCA calculated on the hyperspectral image, by mapping the three principal components to RGB pixel coordinates, shows how the characteristics of the sediments in a cross section can be displayed by clustering their spectral fingerprints, rendered through false colour (Fig. 1).

The morphological and compositional characteristics of the excavated deposits are therefore highlighted by image analysis, used as a support to the stratigraphic reading. The presence of stones, bones or other coarse materials is easily detected. Calcareous stones in the profile are quickly identified. Their dimensions and positioning in the sediment can give a hint about the formation dynamics of those layers. The presence of dry sandy deposits, associated with a random positioning of pebbles, marks a layer of construction debris used in the past century to level off the area. Layer boundaries also appear to be more evident through image analysis, where spectral bands outside the visible range can add information that could help pinpointing invisible patterns. In Figure 1, the limits of the strata appear to be clearer in the right image. This is mostly due to the variability in water absorption of different deposits that is recorded in IR spectra.
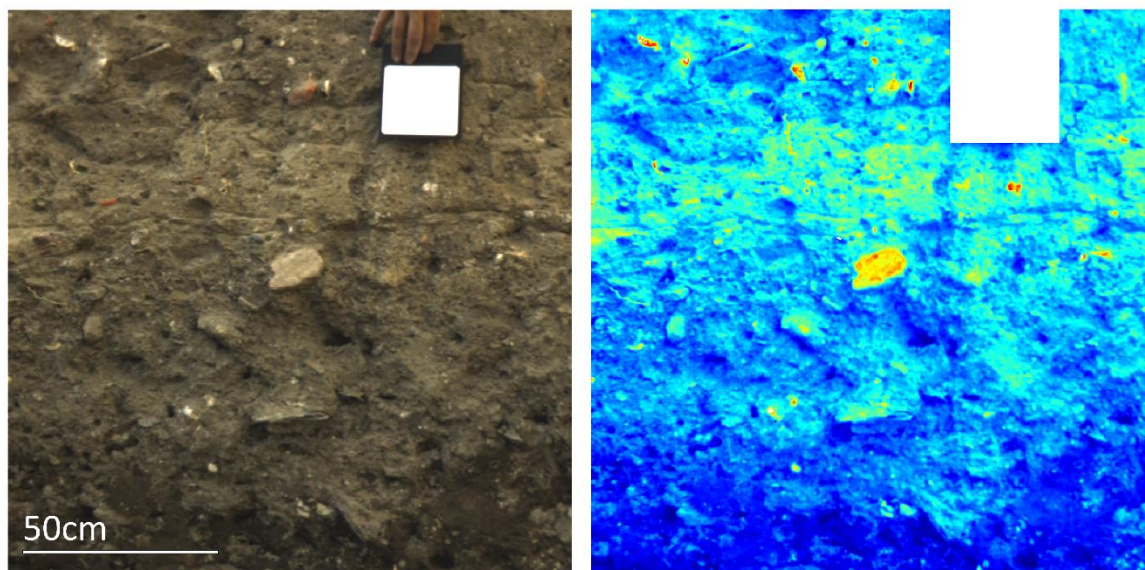
Figure 1 PCA model calculated on a hyperspectral image of an excavation cross-section. On the left, the original image in RGB with the reference white. On the right, the PCA model calculated on the spectral data per pixel (T1).

A similar approach can be applied to the mapping of building materials in monuments. In this case, HSI acquisition allows collecting of spectral data on a large portion of masonry and mapping of single stone blocks based on their spectral fingerprints.

In respect to the medieval (11th century) masonry of the church of San Sisto, in Pisa, the construction technique is characterised by the use of irregular blocks, mainly made in local quartzite, with few blocks made of different lithotypes, being credibly *spolia* from ancient monuments that were available in the area at the moment in which the church was built.

The PCA calculated on the image by using Evince software (Fig. 2) shows a rather clear distinction between quartzite elements and the other lithotypes constituted by calcareous blocks; the HSI mapping enables the fast characterisation of building materials and the lithological mapping, which can help quantifying the rocks within the masonries. This quantitative approach can be quickly adapted to various architectures, widening the sample of building materials provenance, outlining the supply networks of materials and shedding light on building techniques.
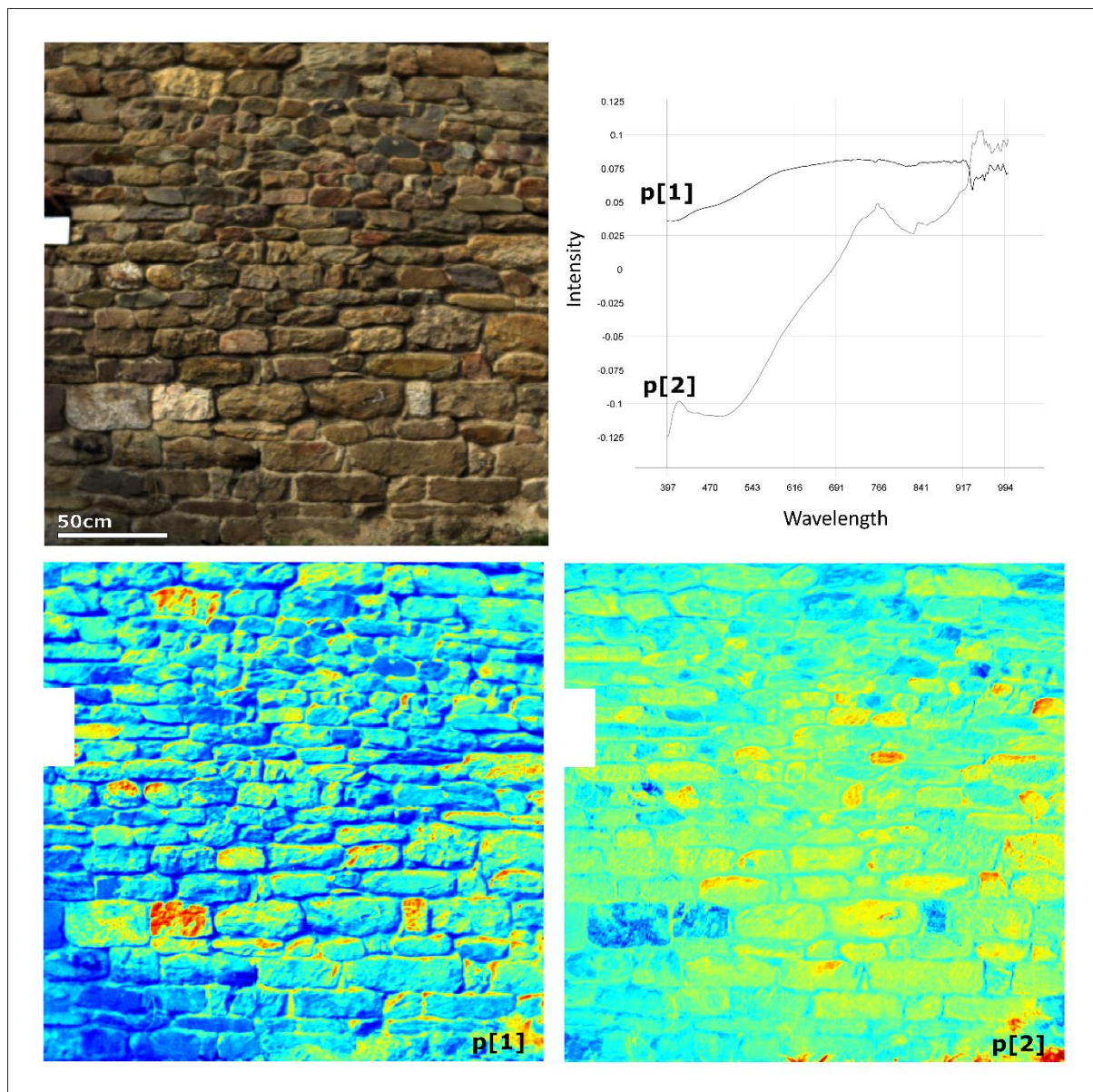
Figure 2 RGB image, loadings and PCA model calculated for p[1] and p[2] on a portion of medieval masonry from the church of San Sisto, Pisa, Italy.

Images taken outdoor could show shadows due to the uncontrolled conditions. Images are often workable even with light shadows; nevertheless, a Python workflow can be applied in order to correct an image lighting. In the case of the medieval masonry of San Sisto (Fig. 3a), an illuminance map was obtained by applying a very strong Gaussian filtering to the results (Fig. 3b). Finally, the shadow was corrected by dividing the spectral image by the illuminance map (Fig. 3c).
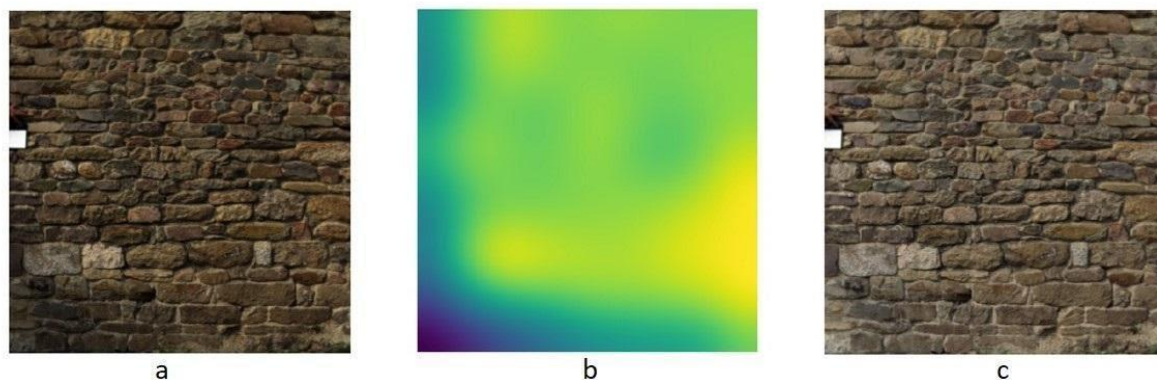
Figure 3 Original hyperspectral image of the medieval masonry of the Church of San Sisto in Pisa, Italy (a), illuminance map of the image (b), shadow-corrected hyperspectral image (c)

3.2 Glazed tiles

One aim of the pilot project «La Fabrique du Caire Moderne» [1] is to study the urban development and architecture in Cairo in the nineteenth and twentieth century by observing the reuse of historic materials from the Mamluk (13th-15th centuries) and Ottoman (16th-18th centuries) periods.

We focused on the Hôtel particulier of Gaston de Saint-Maurice (Volait 2012), a house built in the 1870s by a French aristocrat living in Cairo. Part of the hotel *décors,* made of Iznik ceramic tiles*,* was reused or duplicated to build the house at the present French Embassy. Iznik ceramics were originally produced from the end of the 15th century to the end of the 17th century in Iznik, Western Anatolia (Lane, 1957; Atasoy e Raby, 1989). Similar tiles continued to be produced later in Damascus, Cairo, Rachid, and Tunisia, until the 1750s and possibly afterwards (Theunissen, 2017). Tiles of similar size and patterns can be identified in many monuments and museums in Cairo (sabil-kuttabs, museums, mosques) (Avcıoğlu e Volait, 2017).

The use of the IQ hyperspectral camera on Iznik ceramics tiles was tested with the goal of collecting data about the provenance and reuse of the tiles visible in the house, by obtaining information on the nature of the pigments used. Unsupervised clustering was crucial to better understand the different possible origins of the tiles present in the house and modern Cairo. Acquisitions were made on a selection of tiles under uncontrolled conditions, specifically in a private residence and outdoor. Two sets of hyperspectral images were taken; one set was acquired during the day (under natural light) and the others after sunset (under spotlights: two halogen spots Profoto B1 and B10 with soft boxes or umbrellas at around 1.50 m).

The acquisition was done tile by tile: only one tile per image (the width of the tile corresponded approximately to 450 pixels).

On images acquired, processing was performed using a Python-based workflow, with the aim of applying clustering algorithms (K-means – MacQueen 1967) on the spectra file of the tiles to classify each pixel into groups according to their spectrum. This allowed obtaining an image of the patterns, which facilitated the classification of the tiles by unsupervised clustering (Fig. 4). After importing, the first step was processing the image to remove the colour of the tinted glass on the tile. The pre-processing before clustering consisted of white balancing, the definition of the region of interest and normalisation of the spectrum. An area of the tile without a painted pattern was selected by hand. The area was averaged to get the average spectrum of tinted glass. The spectrum was then divided by the spectrum of each pixel of the image in order to obtain the spectra without the influence of tinted glass (McCluney, 2014).

The spectra of each pixel were then normalised and a clustering algorithm was applied to the image (K-means – MacQueen 1967) in order to separate the different visible colours. The centroids of the clusters correspond to the mean spectrum of each colour. For each colour, the average spectrum is compared to the spectra of known reference pigments by calculating the correlation coefficient between the two spectra. If the correlation coefficient exceeds a threshold value, it is estimated that the pigment is present on the ceramic tile.

Clustering provided very efficient results, and pigments were well separated into different groups. The high spectral resolution of the camera made it possible to separate the red and the broken parts of the ceramic while visually, the colours resemble each other. Likewise, the reflectance spectra of cobalt blue and copper blue could be differentiated into two groups (Cosentino 2014). Cobalt blue-based pigment spectra are recognizable by the characteristic bands at 540, 590 and 640 nm (Llusar et al. 2001) while copper shows a wide absorption band between 500 and 700 nm (Jose & Reddy 2013).

Limits of the IQ camera could be noticed in its low spatial resolution (512 x 512 pixels), which causes a loss of information about sharp details. Fine black contour lines in the tiles resulted poorly detected because of their size, finer than one pixel: the spectrum of the black pigment was therefore mixed with neighbouring pigments and became difficult to segment.
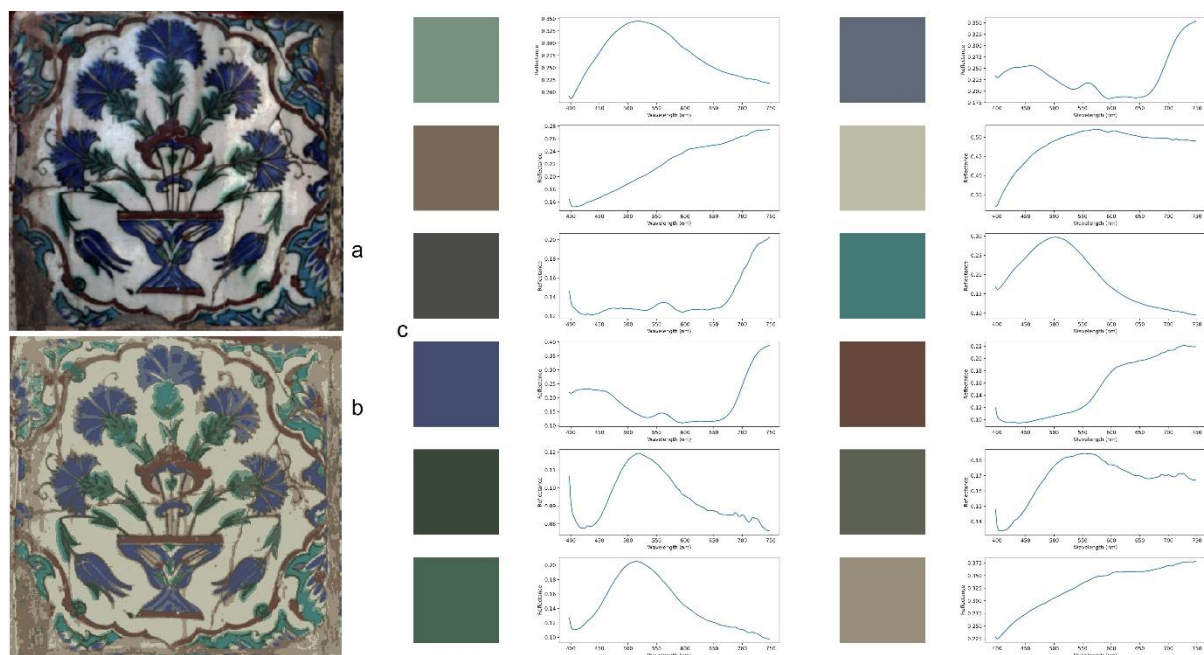
Figure 4 Left: HSI image taken of an Iznik ceramic (converted in RGB for visualization) tile (a). Patterns obtained with unsupervised clustering (b). Mean spectra for each cluster and the corresponding RGB Color (c)

The HSI IQ camera showed to be very practical in this specific context: it made it possible to obtain hyperspectral images in an uncontrolled external environment in a relative short time. If the spatial resolution does not allow sharp details to be analyzed (decoration profiles), the spectral resolution is in this case good enough to achieve automatic pattern recognition within the framework of unsupervised classification. It should be noted, however, that due to the low quality of the images acquired by the IQ in the 900-1000 nm band, the effective range of the HSI camera could be compared to that of a commercial CCD/CMOS infrared photographic camera, which has similar portability with respect to the IQ, can reach extremely high spatial resolution and can acquire a number of spectral images sufficient for pigment identification.

3.3 Roman fresco fragments

A set of fresco fragments found in 1994 during an excavation in the north-western sector of Piazza Duomo (Pisa, Italy) - in an area between the west side of the Monumental Cemetery and the 12th century city walls, near the so-called Lion's Gate (Sorrentino, forthcoming) – were analysed in this study. The painted plasters were part of the decoration of a Roman *domus*, whose architectural structure is still under investigation. The study is part of a doctoral project that aims at outlining the transformations that, from the end of the 2nd century BC to the 5th century AD, affected a vast residential district characterised by *domus* decorated with mosaic floors and painted plasters (Paribeni, et al. 2011). Many fragments of painted plaster were retrieved during several years of excavation, and while their study could now help a better understanding of the building decorations, a holistic approach to old findings could present some issues. The characterisation of a considerable number of fresco fragments was done

by applying HSI as a screening method to distinguish the raw components of pigments and sort the fragments based on the pigment layers recipes. In this case, spectral mapping became a useful tool for classifying archaeological findings based on their spectral response and as a first step for the reconstruction of the decorative apparatus. Since the findings were kept in a laboratory, recording conditions were rather controlled. The fragments of painted plasters were positioned on a table with two halogen lamps set at a 45 degrees angle and the IQ camera in the middle. Images were acquired at a distance of about 50 cm from the target.

The total image, featuring three fragments of painted plasters on a black background, was processed using Evince software. The spectra were mean centred, and a PCA model was calculated in order to explore the data cube and isolate the spectral information pertaining to the frescoes (Fig. 5). Background, labels, and the white reference were excluded from the model, reducing the information to the findings only. The PCA calculated on the fragments shows the mapping of the pigments based on their spectral response. The spectral signature was extracted for each pigment by isolating manually the areas in which the colour layer was even and less affected by weathering. Iron-based pigments, both red and yellow, show similar spectral features, with absorption abdns at 580 anmd 875 nm, but are easily distinguishable by their colour, which reflects in a shift in intensity that allows their classification (Aceto et al. 2014; Linderholm et al., 2015), while the cinnabar spectrum could be distinguished by the characteristic inflection point at 586 nm (Vetter & Schreiner, 2014) (the chemical characterisation of pigments was verified by using the portable XRF Elio by Bruker). In this case, image mapping could allow an easy grouping of iron-based and cinnabar pigments on a series of small samples with a flat surface, fostering a faster classification of excavation findings, useful for the interpretation of the features excavated over a long time-span.
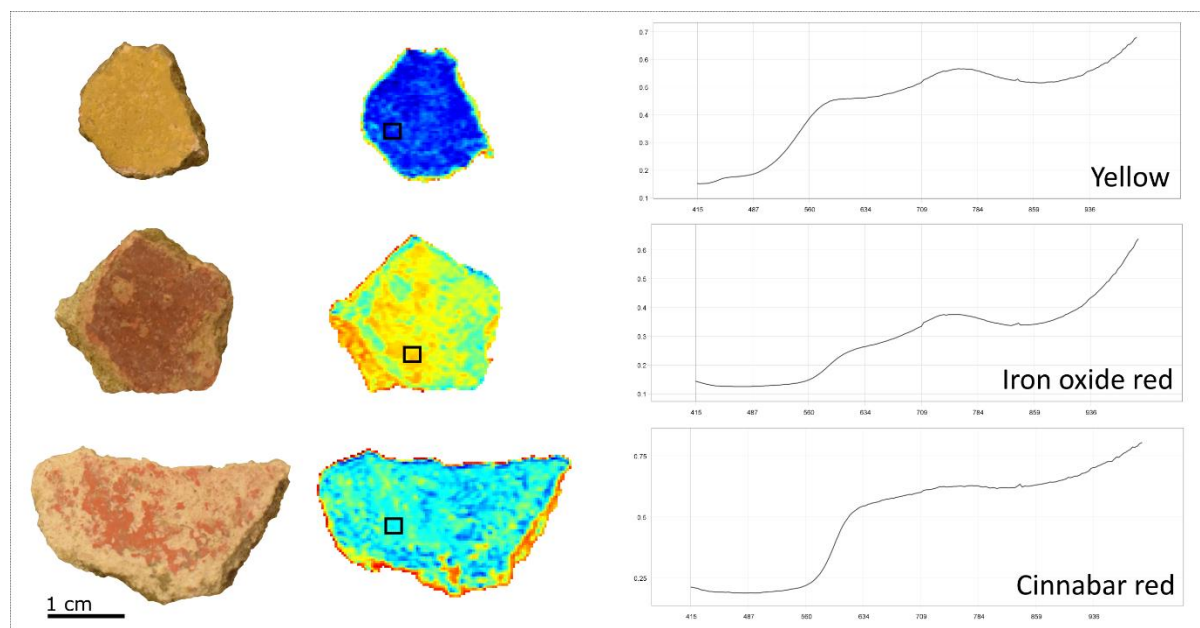
Figure 5 fresco fragments from the excavation in Piazza dei Miracoli, Pisa (Italy). From left: RGB images of the single fragments, PCA model calculated on the HSI, pigments spectral fingerprints.

3.4 Tapestry/textiles

Fragments of textiles are not frequently recovered in archaeological contexts. These fragile materials can be preserved only in specific conditions and archaeological textiles are often very damaged by post depositional processes. Considering these aspects, an image-based approach to the mapping of fibers and dyes is preferrable in order to explore the objects's features (Al-Gaoudi & Iannaccone 2021; Peruzzi et al. 2021; Žemaitytė et al. 2006) while knowing that "non-planarity" of the textile fibre can affect the signal-to-noise ratio rather than the "quality" of the fibre itself (De La Codre et al. 2021b). In this case study we investigated a tapestry with different imaging techniques in order to show how this approach could be applied to other kinds of textiles. The tapestry studied is a "Verdure" (landscape representation with a big size of (7.32 x 3.44 m), a speciality of Aubusson Royal Manufacture produced mainly for export (Bertrand 2013). It was commissioned by the Count Brühl, Prime Minister of August III, King of Poland. It has a very high and fine quality weaving and a superior quality dyeing. It is of particular interest, as the lining of the back that protected it from light was removed in November 2018, pending restoration. The colours on the back are less exposed to light and better preserved. This tapestry gives the rare opportunity to study the materials (fibres, dyes and mordants) in both faces, so at different degradation states, by non-invasive methods (Clementi et al. 2014; Melo e Claro 2010; de La Codre et al. 2021a; Mounier *et al*., 2020). Hyperspectral imaging was used to identify and map the dyes (VIS) and textiles (SWIR). The tapestry was illuminated with two halogen lamps oriented at 45° at a working distance of 1.1m to have a global image. Images on the same spots were also acquired through a Vis-NIR CCD camera (Specim HS-XX-V10E), with a 1600 x 840 pixels resolution (pixel size: 8 x 8 µm), a 2.8 nm spectral resolution and a spectral wavelength range from 400 to 1000 nm. For the HS-XX-

V10E camera, one pixel corresponded in real size on the tapestry to 0.38 mm (surface mapped: 61 x 32 cm^2) while it is 1.05 mm for the IQ camera (surface mapped: 54 x 54 cm^2).

With both the IQ camera and the Specim HS-XX-V10E, spectral IDAQ software provided data acquisition, storage, and calibration. The treatment of the data cube was performed with ENVI 5.2+IDL software. Spectra are the result of an average window of 10 x 10 pixels for both cameras to limit the background noise, improve the readability of the spectra and, therefore, the interpretation of the bands. As expected, images obtained through the HSI-IQ camera showed a lower quality than those of the HS-XX-V10 (Fig. 6 a & b). Images appeared blurry because of the low resolution of the system. Nonetheless, the averaged spectra were workable.

For the identification of the dyes, three examples were chosen on red (Fig. 6c), green (Fig. 6d) and yellow (Fig. 6e) zones of the same object, namely a flower. In both cases, IQ and HS-XX-V10E, the reflectance spectra obtained for the red could be easily attributed to madder, thanks to the two absorption bands at 510 and 540 nm (Aceto *et al.,* 2014). When the madder concentration is very high, these bands disappear, and an inflection point at 560 nm shows up (Tamburini & Dyer, 2019). The resolution of the two cameras seems to be good enough to characterise a red dye. We note that the noise of the HSI-VNIR images below 450 nm and above 900 nm is even higher than the one of the HSI-IQ, which is not surprising given the fact that the two cameras share the same push-broom technology. For the green leaf of the flower, we observe that the two spectra are comparable, and the shape of the curve suggests a dye mixture. The inflection point at about 666 nm indicates the presence of indigo, a blue dye commonly used in tapestries. Thanks to the old treatises (Hellot 1750; Du Fay, 1737; Macquer P-J, 1761), which describe the dyes recipes, we know that to obtain green, the textile fibre is first dyed with indigo and then with a yellow flavonoid dye such as weld, or dyer's broom. The presence of a yellow flavonoid can be demonstrated by the reflection band between 450 to 660 nm. In thiscase, both cameras can give the same spectra, allowing the identification of the dyes.

The identification of the yellow dye is not simple. Yellow dyes are known to be fragile to light; most of the time, they lose their colour and are difficult to characterise (de La Codre et al. 2021). In fact, even if the same treatment was applied in all the spectra, the spectra obtained with the two HSI cameras are not equivalent for the yellow dye. The difference can be explained by the different spatial resolutions of the two cameras. In the case of the HSI-VNIR, the pixel size is about 8 x 8 μm, whereas, for the HSI-IQ, it is 17.58 x 17.58 μm. An average of 10 x 10 pixels was applied to reduce the noise ratio and improve the spectrum. This corresponds to an area in the tapestry of 1.44 mm² for the HSI-VNIR camera and 12.1 mm² for the IQ camera. By averaging the spectra, the analysis area for the IQ camera is 8.4 times larger than the one of the HS-XX-V10E; this would improve the signal to noise ratio, resulting in a smoother spectrum for the IQ camera. The difference observed between the spectra acquired with the two cameras can also be explained by the fact that the analysed zone was very small (yellow pistil of the flower), and a contribution of the red dye next to the yellow on the tapestry cannot be excluded, in the case of the low spatial resolution IQ camera.
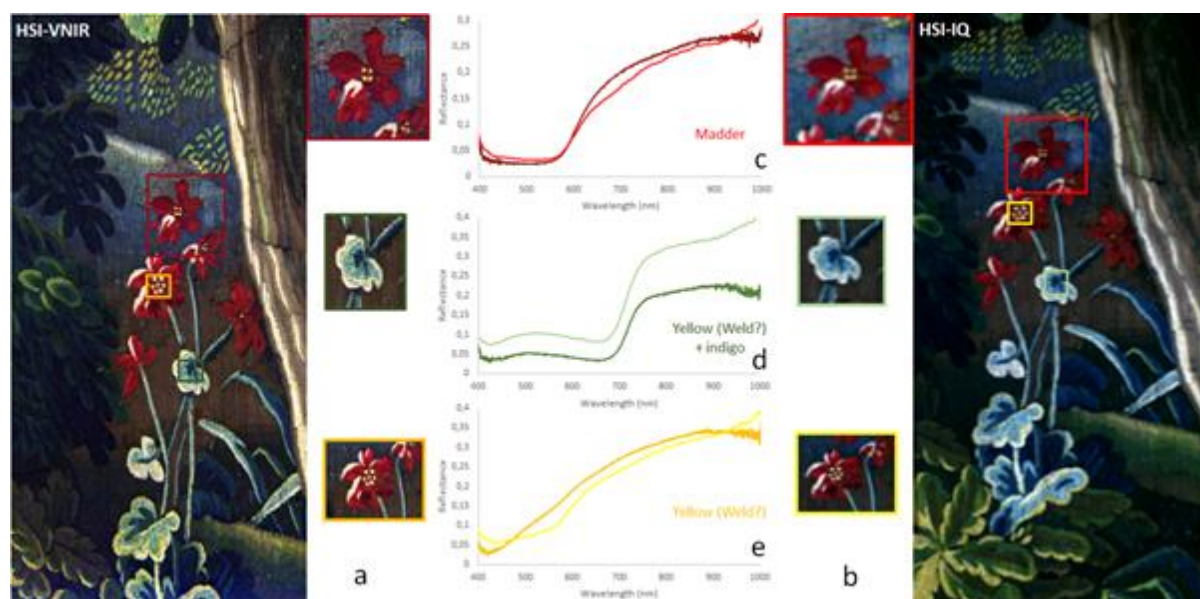
Figure 6 Hyperspectral images (a & b) and reflectance spectra (c, d, e) in the visible range (400-1000 nm) obtained with the HSI-VNIR (a & darker spectra) and the HSI-IQ (b & lighter spectra) on a 18th C. tapestry kept at the Cité Internationale de la Tapisserie

The IQ camera seems to work well when the dye presents a characteristic spectrum with a specific and straightforward band (such as indigo), in other words, for well-known dyes. The poor spatial resolution might give problems when the camera is used on small and/or uneven samples. In the case of large and flat homogeneous surfaces, the IQ camera can be very effective for the identification of the pigment, as demonstrated here by the blue and red dyes examples. In those cases, the reflectance spectra of the IQ camera appear better resolved than the one of the HSI –VNIR. This can be explained by the fact that the analysed area is larger than the one of the VNIR camera; therefore, the signal/noise ratio is better for the IQ camera. However, while analysing strongly inhomogeneous samples, the results may be unsatisfactory. In the presented application, the woolen or silky threads are intermingled and a precision of the order of the size of the fibre (around 40 µm for wool and 10 µm for silk) would be necessary for obtaining pure spectra. The high-resolution HS-XX-V10E VNIR camera is more suited for this type of application. It should also be considered that all the techniques based on the spectral determination of the diffuse reflectance of the samples (Hyper-/Multispectral imaging, Fiber-Optics Reflectance Spectroscopy, FORS (Clark et al., 1984), etc.) become less and less performant when applied to degraded, mixed and/or layered dyes or pigments, which would produce a deviation of the reflectance spectrum with respect to the one characterising the pure dye/pigment. Unfortunately, degraded, mixed, and layered dyes & pigments are commonly found in Cultural Heritage and Archaeology applications; this fact strongly suggests the use of other, more discriminant methods (micro-Raman spectroscopy, X-Ray Fluorescence, Laser-Induced Breakdown Spectroscopy for pigments and FTIR, High Performance Liquid Chromatography, mass spectrometry or fluorimetry for dyes) (Veneranda et al., 2018). Most of these methods can be implemented in situ with portable instrumentation and would, in general, provide, especially if used together, clear answers for the identification of the dyes/pigments under analysis.

4 NIR range and outdoor conditions

The case studies considered in the present work highlighted some issues related to the quality of the spectral images at the extremes of the instrument sensitivity when images are acquired in outdoor conditions. In fact, it has been observed that while the quality of the images – besides their relatively low resolution, corresponding to about 0.25 MegaPixels – is generally acceptable in the central part of the working range, the images acquired in the Violet/Blue band (from to 400 to 450 nm) and in the Near Infrared band between 900 and 1000 nm are quite noisy.

For example, as shown by the PCA calculated on the San Sisto wall masonry images (see Fig. 2 for t[1] and t[2]), at the extremes of the instrument sensitivity, the spectrum is poor in quality, excluding the most informative region of the VIS-NIR spectrum. Nevertheless, in this case, the results are quite acceptable since the principal components of the masonry's constituents are dominated by the spectral regions < 900 nm. In the range 900-1000 nm, the reason of the observed noise has to be attributed to the lightning/scattering effect, which seems to be caused by the atmospheric absorption bands in the range 920-980 nm (Goody & Young, 1995). Since conventional CCD-based hyperspectral cameras do not suffer the same problems, that might be considered structural of the IQ camera and its detector sensitivity; Behmann et al. (2018) proposed as a solution to use spectral flattening filter and increase the integration time when using the IQ camera under natural light.

It is interesting to note that the poor quality of the NIR spectrum between 900 and 1000 nm depends a lot on the light environment, as confirmed by a test carried out on glazed ceramic tiles from Iznik, analysed under different conditions in order to compare spectra acquired in both artificial and natural light. Photographs of an Iznik tile were taken in a completely closed room (dry and controlled environmental conditions of the laboratory) with two halogen lamps. The selected tile was painted using the same pigments as in the tiles photographed outdoor in Cairo.

The results in Figure 7 show that in open air and natural light, the spectrum is very noisy, even after spatial averaging over the region of interest of 5x5 pixels. We can also notice a sharp characteristic peak of H_2O absorption between 925 and 970 nm (Behmann et al., 2018; Goody and Yung, 1995).

In the case of measurement in a dry environment, the H_2O absorption peak disappears (Behmann et al., 2018), and the noise in the IR region is attenuated: it is possible to eliminate it by carrying out a spatial averaging even if it remains slightly visible in the spectra of the single pixels.
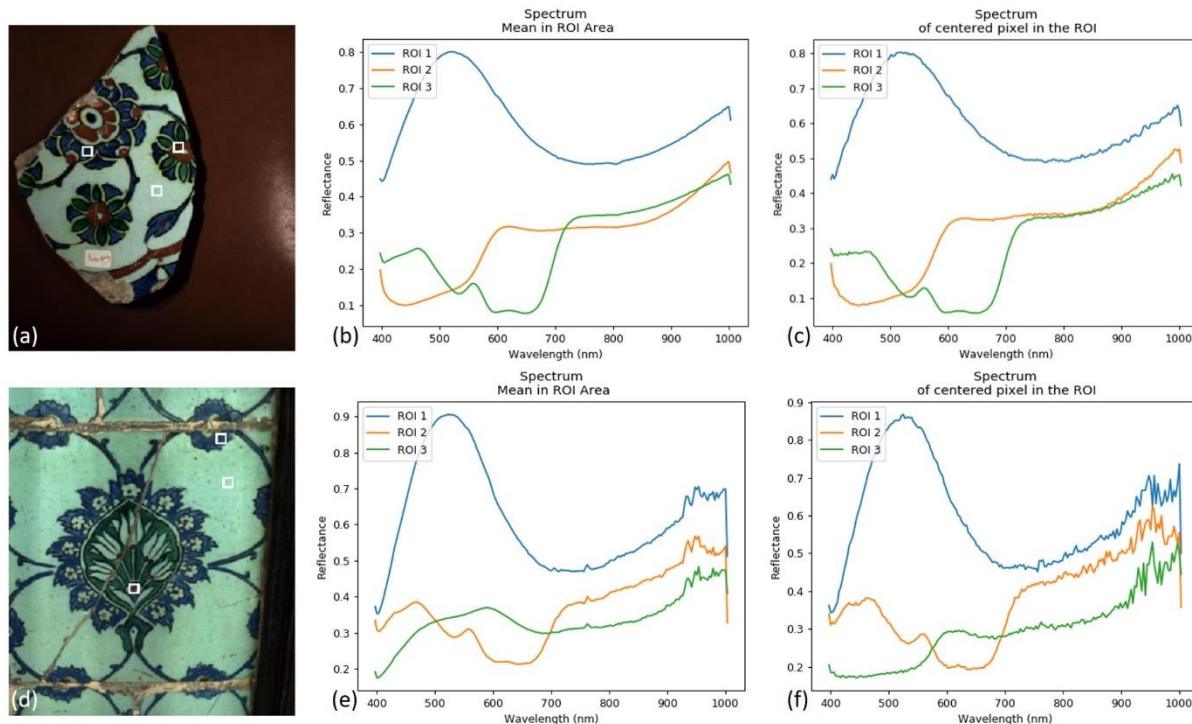
Figure 7: Comparison of the spectral image of a fragment of Iznik ceramic in controlled dry environment and under artificial light (a) and a tile containing the same pigments in open air, under natural light (d). For the regions of interest containing the blue and red pigments, as well as the background, we observe the spectrum averaged over 5 x 5 pixels in dry controlled environment under artificial (b) and in open air under natural (e) light. Likewise, we observe the spectrum of these elements in controlled dry environment and under artificial light (c) and in open air under natural light (f) in the case of a single pixel (no averaging).

Even in measurements performed in open air, the effect of H_2O absorption can be moderated for well-illuminated samples highly reflecting in the Infrared region. Figure 8 shows an image taken with the IQ camera at 1000 nm on a facade made by marble blocks at the Pisa Cathedral, in direct (a) and indirect (b) illumination. Both the images are rather noisy, but the image taken under direct solar illumination is still workable (possibly using moderate spatial averaging) while the one corresponding to lower environmental light conditions suffers the presence of a structured noise (horizontal darker lines, see figure (c) for a detail) which gradually decreases al lower wavelengths, to almost disappear around 900 nm. However, even in the most favourable conditions, it is important to temper the effect of averaging. Indeed, the resolution of the IQ camera is already very low. For attempting a classification of the materials with coarse details, we can tolerate a relatively low signal-to-noise ratio and even losing details by averaging over a 5 x 5 area (thus reducing the resolution of the camera to a mere 0.01 Mpixels). On the other hand, when the details are important, spatial averaging and noise on the measurement may result less tolerable. In that case, the low sensitivity at the extremes of the spectral range can be reduced by using an illuminator providing a lot of blue and IR radiation. Then the reflected signal would be higher, and the quality of the images would be better. But in most of cases, obtaining a strong signal in the blue and IR is not easy, hence the problems of structured noise that makes difficult the use of the system for the analysis of fine details.

Figure 8: Comparison of the spectral images taken with the IQ camera at 1000nm on the marbles of the Pisa cathedral in (a) direct solar illumination; (b) indirect illumination. Figure (c) shows a detail of the structured noise affecting all the spectral region from 900 to 1000 nm.

5 Conclusions

This contribution retraces the steps of an international and interdisciplinary exchange of knowledge on ultraportable HSI undertaken among institutions with different research goals but a shared interest in developing effective field techniques for fostering research on archaeological materials.

The case studies reported do not cover all the possible applications of Hyperspectral Imaging in archaeological studies; however, some general considerations can be drawn for the applications in which a small ultraportable camera can be superior to other more conventional solutions.

Specifically talking about the Specim IQ device, the spectral range of 600 nm of the camera (from 400 to 1000 nm), divided into 204 overlapping bands, seems not fully exploitable; the number is still considerable, but such a remarkable spectral resolution is obtained at the cost of a poor spatial resolution. This is undoubtedly a limit when there is a need for mapping smaller details, while the compromise can be advantageous when a large number of spectral bands is actually essential to the specific study. In all the other cases in which spatial resolution is not an issue, a rugged device such as the Specim IQ can be considered a valuable instrument for *in situ* analysis. Advantages with the use of an ultraportable camera are surely its extreme portability and rugged hardware, as mentioned above, that makes it easy to transport the instrument and use it in various conditions. This is particularly suited when moving abroad in countries with special customs requirements when measuring targets that are placed in peculiar places with limits or difficulties in instruments positioning or challenging environmental conditions. Illumination in outdoor conditions can be a critical aspect imprinting the quality of the spectrum at the extremes of the instrument sensitivity; however, appropriate corrections and average tools might improve spectral images, especially in the range 900-1000 nm.

The spectral range of the camera is well suited for mapping pigments and dying, allowing the fast screening of a large number of fragmented artefacts or an overview of fragile and composite objects. For these applications, an ultraportable instrument could be used in museums or excavation storage spaces, allowing the collection of preliminary data that can be used for speeding up the classification of artefacts or for a first mapping of an object's features. The use of HSI in other contexts, such as

excavations and surveys, must rely on a different approach. While most spectral bands that are characteristic of minerals are located in the SWIR region, soils can be characterised in the IR by using proxies. In this case HSI is useful to make a better estimation of those parameters (colour, composition and particle size, inclusions) that are used as a discriminant when interpreting archaeological stratigraphy. Both in the case of soil profiles and masonries, the processing of hypercubes is similar to what is done in multi-hyperspectral satellite imaging, especially regarding the use of water absorption in the target to highlight otherwise invisible patterns.

While data collected with these techniques can be difficult to process due to the large size of the files, commercial software are available to create semi-automated classifications, as well as script pipelines that can be modified according to specific needs.

The widespread use of HSI as a screening technique in fieldwork could effectively help a broader and more comprehensive study of archaeological deposits and materials. Sharing data gathered through imaging could be useful for building online collaborative libraries, support interdisciplinary in-field teaching while tearing down hindrances between field archaeology and laboratory archaeology, and contributing to make archaeological sciences a truly transdisciplinary and ethical endeavor (Milek 2018).

Acknowledgements

Reference list

Aceto, M., A. Agostino, G. Fenoglio, A. Idone, M. Gulmini, M. Picollo, P. Ricciardi, and J. K. Delaney. 2014. "Characterisation of colourants on illuminated manuscripts by portable fibre optic UV-visible-NIR reflectance spectrophotometry." *Analytical Methods* 6(5): 1488-1500.

Adinolfi G., R. Carmagnola, M. Cataldi, L. Marras, and V. Palleschi. 2019. "Recovery of a lost wall painting at the Etruscan Tomb of the Blue Demons in Tarquinia (Viterbo, Italy) by multispectral reflectometry and UV fluorescence imaging" *Archaeometry* 61(2): 450–458.

Al-Gaoudi, H. A., and R. Iannaccone. 2021. «Multiband imaging techniques incorporated into the study of dyed ancient Egyptian textile fragments.» *International Journal of Conservation Science* 12 (3): 893–906.

Atasoy, N., and J. Raby. 1989. *Iznik. The Pottery of Ottoman Turkey*. London.

Avcıoğlu, N., and M. Volait. 2017. "Jeux de miroir": Architecture of Istanbul and Cairo from Empire to Modernism". In Barry F. and N. Gulru (eds.) *A Companion to Islamic Art and Architecture*. Oxford: Wiley-Blackwell.

Baldridge, A. M., S. J. Hook, C. I. Grove, e G. Rivera. 2009. «The ASTER spectral library version 2.0». *Remote sensing of Environment* 113 (4): 711–15.

Behmann, J., K. Acebron, D.Emin, S.Bennertz, S. Matsubara, S. Thomas, D. Bohnenkamp, M. T. Kuska, J. Joussila and H. Salo, U. 2018. "Specim IQ: evaluation of a new, miniaturized handheld hyperspectral camera and its application for plant phenotyping and disease detection." *Sensors*, 18(2): 441.

Bertrand, P. 2013. *Aubusson, tapisseries des Lumières: splendeurs de la Manufacture royale, fournisseur de l'Europe au XVIIIe siècle*. Snoeck.

Campana, S., and M. Forte. 2006. *From space to place*. BAR International Series 1568.

Choi, Y. J., J. Lampel, S. Fiedler, D. Jordan, and T. Wagner. 2020. "A new method for the identification of archaeological soils by their spectral signatures in the vis-NIR region". *Journal of Archaeological Science: Reports* 33: 102553.

Clark, R.N., and T.L. Roush. 1894. "Reflectance spectroscopy: quantitative analysis techniques for remote sensing applications" *Journal of Geophysical Research* 89 (B7): 6329-6340.

Clark, Roger N., G. A. Swayze, A. J. Gallagher, T. VV King, and W. M. Calvin. 1993. «The us geological survey, digital spectral library: Version 1 (0.2 to 3.0 um)». Geological Survey (US).

Clementi, C., G. Basconi, R. Pellegrino, and A. Romani. 2014. «Carthamus tinctorius L.: A photophysical study of the main coloured species for artwork diagnostic purposes». *Dyes and Pigments* 103: 127–37.

Cucci, C., J. K. Delaney, and M. Picollo. 2016. «Reflectance hyperspectral imaging for investigation of works of art: old master paintings and illuminated manuscripts». *Accounts of chemical research* 49 (10): 2070–79.

Cosentino, Antonino. 2014. "FORS Spectral Database of Historical Pigments in Different Binders" *e-conservation Journal* 2: 53–65

Cucci, C., M. Picollo, L. Chiarantini, G. Uda, L. Fiori, B. De Nigris, and M. Osanna. 2020. «Remote-sensing hyperspectral imaging for applications in archaeological areas: Non-invasive investigations on wall paintings and on mural inscriptions in the Pompeii site». *Microchemical Journal* 158: 105082.

De La Codre, H., C. Marembert, P. Claisse, F. Daniel, R. Chapoulie, L. Servant and A. Mounier. 2021a. "Non- invasive characterization of yellow dyes in tapestries of the 18th century: Influence of composition on degradation". *Color Research & Application*, 46(3): 613-622.

De La Codre, H., F. Daniel, R. Chapoulie, L. Servant, and A. Mounier. 2021b. «Investigating the Materials Used in Eighteenth-Century Tapestries from the Three French Royal Manufactories: Inputs of Hyperspectral Approaches». *The European Physical Journal Plus* 136 (11): 1193. https://doi.org/10.1140/epjp/s13360-021-02184-3.

Du Fay 1737. Observations physiques sur le meslange [sic] de quelques couleurs dans la teinture. In: *Histoire de l'Académie Royale Des Sciences Avec Les Mémoire de Mathématique & de Physique Pour La Même Année.* Imprimerie de Du Pont. Imprimerie Royale; 1737:253-268.

Gabrieli, F., K. A. Dooley, M. Facini, and J. K. Delaney. 2019. «Near-UV to mid-IR reflectance imaging spectroscopy of paintings on the macroscale». *Science advances* 5 (8): eaaw7794.

Geladi, P., and H. F. Grahn. 1996. "Multivariate image analysis". In *Encyclopedia of Analytical Chemistry*. John Wiley & Sons.

Goody, R. M., and Yung, Y. L. 1995. *Atmospheric radiation: theoretical basis*. Oxford university press.

Grahn, H., and P. Geladi. 2007. *Techniques and applications of hyperspectral image analysis*. John Wiley & Sons.

Grifoni, E., B. Campanella, S. Legnaioli, G. Lorenzetti, L. Marras, S. Pagnotta, V. Palleschi, F. Poggialini, E. Salerno, E., and A. Tonazzini, 2019. "A New Infrared True-Color Approach for Visible-Infrared Multispectral Image Analysis". *Journal of Computing and Cultural Heritage,* 12(2) Art. 8 1-11

Hellot, J. 1750. *L'art de la teinture des laines et des étoffes de laine en grand et petit teint. Avec une instruction sur les déboüillis*, Pissot et Jean Thomas Herissant

Hodder, I., and A. Berggren. 2005. *At the Trowel's Edge: An Introduction to Reflexive Field Practice in Archaeology*. Westview.

Jose, S., and R. Mundlapudi Lakshmipathi. 2013. «Lanthanum–Strontium Copper Silicates as Intense Blue Inorganic Pigments with High near-Infrared Reflectance». *Dyes and Pigments* 98 (3): 540–46. https://doi.org/10.1016/j.dyepig.2013.04.013.

Koehler, Frederick W., Eunah Lee, L. H. Kidder, and E. Neil Lewis. 2002. «Near infrared spectroscopy: the practical chemical imaging solution». *Spectroscopy Europe* 14 (3): 12–19.

Lane, A. 1957. "The ottoman pottery of Isnik". *Ars Orientalis*, 247–81.

Legnaioli S., E. Grifoni, G. Lorenzetti, L. Marras, L. Pardini, V. Palleschi, E. Salerno, and A. Tonazzini. 2013a. "Enhancement of hidden patterns in paintings using statistical analysis" *Journal of Cultural Heritage* 14(3): S66–S70.

Legnaioli S., G. Lorenzetti, G. H. Cavalcanti, E. Grifoni, L. Marras, A. Tonazzini, E. Salerno, P. Pallecchi, G. Giachi, and V. Palleschi. 2013b. "Recovery of archaeological wall paintings using novel multispectral imaging approaches" Heritage Science 1 (1): 1-9.

Liang, H. 2012. «Advances in multispectral and hyperspectral imaging for archaeology and art conservation». *Applied Physics A* 106 (2): 309–23.

Linderholm, J., J. A. Fernández Pierna, D. Vincke, P. Dardenne, and V. Baeten. 2013. "Identification of fragmented bones and their state of preservation by using near infrared hyperspectral image analysis". *Journal of Near Infrared Spectroscopy* 21 (6): 459–66.

Linderholm, J., P. Geladi, and C. Sciuto. 2015. "Field-based near infrared spectroscopy for analysis of Scandinavian Stone Age rock paintings". *Journal of Near Infrared Spectroscopy* 23 (4): 227–36.

Linderholm, J., P. Geladi, N. Gorretta, R. Bendoula, and A. Gobrecht. 2019. "Near infrared and hyperspectral studies of archaeological stratigraphy and statistical considerations". *Geoarchaeology* 34 (3): 311–21.

Llusar, M., A. Forés, J. A. Badenes, J. Calbo, M. A. Tena, and Guillermo Monrós. 2001. «Colour Analysis of Some Cobalt-Based Blue Pigments». *Journal of the European Ceramic Society* 21 (8): 1121–30. https://doi.org/10.1016/S0955-2219(00)00295-8.

MacQueen, J. 1967. Some methods for classification and analysis of multivariate observations. In *Proceedings of the fifth Berkeley symposium on mathematical statistics and probability*, 1 (14), pp. 281-297.

Macquer P-J. 1761. *Art de La Teinture En Soie.* Desaint.

Masini, N., and F. Soldovieri. 2017. *Sensing the Past*. Springer.

McCluney, W. R. 2014. *Introduction to radiometry and photometry*. Artech House.

Melo, M. J., and A. Claro. 2010. "Bright light: microspectrofluorimetry for the characterization of lake pigments and dyes in works of art". *Accounts of chemical research* 43 (6): 857–66.

Milek, K. 2018. «Transdisciplinary Archaeology and the Future of Archaeological Practice: Citizen Science, Portable Science, Ethical Science». *Norwegian Archaeological Review* 51 (1–2): 36–47.

Mounier A., and F. Daniel, 2017, Pigments & Dyes in a collection of medieval illuminations (14th – 16th century), *Color Research and Applications* 42, pp. 807-822. DOI 10.1002/col.22146.

Mounier A., H. De la Codre, C. Marembert, P. Claisse, and F. Daniel, 2020, "Rediscover the faded colours of an 18th century tapestry kept in the Cité Internationale de la tapisserie in Aubusson (France)", In *Proceedings of the International Colour Association (AIC) symposium Natural Colours – Digital Colours* 20, 24-26/11/2020, Avignon, France, 178-185.

Mounier A., C. Denoël, and F. Daniel, 2016, Hyperspectral imaging on three French medieval illuminations of the XVI century (Treasury of Bordeaux Cathedral, France), COLOURS2015, Evora, Portugal, 24-26 sept. 2015, *Color Research and Application Journal*, 41 (3), DOI: 10.1002/col.22042.

Mounier A., G. Le Bourdon, C. Aupetit, S. Lazare, J. Perez-Arantegui, D. Almazan, J. Aramendia, N. Prieto-Taboada, S. Fdez-Ortiz de Vallejuelo, and F. Daniel. 2018, Red and blue colours on 18th-19th century Japanese woodblock prints: In situ analyses by spectrofluorimetry and complementary noninvasive spectroscopic methods, *MicroChemical Journal* 140, pp129-141. DOI:10.1016/j.microc.2018.04.023.

Parcak, S. H. 2009. *Satellite remote sensing for archaeology*. Routledge.

Paribeni, E., L. Parodi, F. Marra, S. Genovesi, and D. Stiaffini. 2011. "Un quartiere residenziale di Pisa romana (Periodo II)". In Paribeni E. and A. Alberti (eds.) *Archeologia in Piazza dei Miracoli. Gli scavi 2003-2009*: 71-166.

Parish, R. M. 2011. "The application of visible/near- infrared reflectance (VNIR) spectroscopy to chert: A case study from the Dover Quarry sites, Tennessee". *Geoarchaeology* 26 (3): 420–39.

Peruzzi, G., C. Cucci, M. Picollo, F. Quercioli, and L.o Stefani. 2021. «Non-Invasive Identification of Dyed Textiles by Using VIS-NIR FORS and Hyperspectral Imaging Techniques». *Cultura e Scienza Del Colore - Color Culture and Science* 13 (01): 61–69. https://doi.org/10.23738/CCSJ.130207.

Prats-Montalbán, J. M., A. De Juan, and A. Ferrer. 2011. "Multivariate image analysis: a review with applications". *Chemometrics and Intelligent Laboratory Systems* 107 (1): 1–23.

Prinsloo, L. C., W. Barnard, I. Meiklejohn, and K. Hall. 2008. "The first Raman spectroscopic study of San rock art in the Ukhahlamba Drakensberg Park, South Africa". *Journal of Raman Spectroscopy: An International Journal for Original Work in all Aspects of Raman Spectroscopy, Including Higher Order Processes, and also Brillouin and Rayleigh Scattering* 39 (5): 646–54.

Rossel, RA Viscarra, T. Behrens, E. Ben-Dor, D. J. Brown, J. A. M. Demattê, Keith D. Shepherd, Z. Shi, B. Stenberg, A. Stevens, e Vj Adamchuk. 2016. «A global spectral library to characterize the world's soil». *Earth-Science Reviews* 155: 198–230.

Salerno E., A. Tonazzini, E. Grifoni, G. Lorenzetti, S. Legnaioli, M. Lezzerini, and V. Palleschi. 2014. "Analysis of Multispectral Images in Cultural Heritage and Archaeology". *J. Appl. Laser Spectrosc.* 1: 22–27.

Schmidt, P., V. Léa, Ph Sciau, and F. Fröhlich. 2013. «Detecting and quantifying heat treatment of flint and other silica rocks: a new non- destructive method applied to heat-treated flint from the Neolithic Chassey culture, southern France». *Archaeometry* 55 (5): 794–805.

Sciuto, C., D. Allios, R. Bendoula, A. Cocoual, M.-E. Gardel, P. Geladi, A. Gobrecht, N. Gorretta, N. Guermeur, and S. Jay. 2019. "Characterization of building materials by means of spectral remote sensing: The example of Carcassonne's defensive wall (Aude, France)". *Journal of Archaeological Science: Reports* 23: 396–405.

Sciuto, C., P. Geladi, L. La Rosa, J. Linderholm, and M. Thyrel. 2018. "Hyperspectral Imaging for Characterization of Lithic Raw Materials: The Case of a Mesolithic Dwelling in Northern Sweden". *Lithic Technology*, 1–14.

Sorrentino, G. Forthcoming. "Gli scavi del settore nord-occidentale di Piazza del Duomo (Pisa). Nuovi dati per la ricostruzione del paesaggio urbano in epoca romana". In Fabiani F. and G. Gattiglia (eds.), Paesaggi urbani e rurali in trasformazione. Contesti e dinamiche dell'insediamento letti alla luce della fonte archeologica. Atti della Giornata di Studi dei Dottorandi in Archeologia (Pisa, 22 Novembre 2019). Archaeopress.

Tamburini D, and J. Dyer, 2019. "Fibre optic reflectance spectroscopy and multispectral imaging for the non-invasive investigation of Asian colourants in Chinese textiles from Dunhuang (7th-10th century AD)". *Dyes and Pigments* 162: 494-511.

Theunissen, H. 2017. "The Ottoman Tiles of the Fakahani Mosque in Cairo". *Journal of the American Research Center in Egypt* 53: 287–330.

Triolo, P., Marras, L., Adinolfi, G, Carmagnola, R., Legnaioli, S., Raneri, S., Palleschi, V. 2020. "Imaging for Cultural Heritage and Archaeology". 2020 IMEKO TC-4 International Conference on Metrology for Archaeology and Cultural Heritage: 512-516.

Vandenabeele, Peter, e Mary Kate Donais. 2016. «Mobile spectroscopic instrumentation in archaeometry research». *Applied Spectroscopy* 70 (1): 27–41.

Veneranda, M., S. Fdez-Ortiz de Vallejuelo, N. Prieto-Taboada, M. Maguregui, I. Marcaida, H. Morillas, A. Martellone, B. de Nigris, M. Osanna, K. Castro, and J.M. Madariaga. 2018. "In-situ multi-analytical characterization of original and decay materials from unique wall mirrors in the House of Gilded Cupids, Pompeii" *Heritage Science* 6 (1): 40.

Vetter, W., and M. Schreiner. 2014. "A Fiber Optic Reflection-UV/Vis/NIR-System for Non-destructive Analysis of Art Objects". *Advances in Chemical Science* 3 (1): 7–14.

Volait, M. 2012. *Maisons de France au Caire: le remploi de grands décors mamelouks et ottomans dans une architecture moderne*. Institut français d'archéologie orientale.

Žemaitytė, R., V. Joaidienė, R. Milašius, S. Stanys, and R. Ulozaitė. 2006. «Analysis and identification of fibre constitution of archaeological textiles». *chemical analysis* 2: 7–10.